Biochemistry

 Volume 37, Number 13 March 31, 1998

New Concepts in Biochemistry

Interdigitated Solenoid Model for Compact Chromatin Fibers†

Joan-Ramon Daban* and Antonio Bermúdez

Departament de Bioquímica i Biologia Molecular, Facultat de Ciències, Universitat Autònoma de Barcelona, 08193-Bellaterra, Barcelona, Spain

Received December 18, 1997

Our previous electron microscopy (*1*) and electrophoretic (*2*) studies of small chromatin fragments from chicken erythrocytes have shown that, in the presence of 1.7 mM Mg^{2+}, these fragments form helical fibers which are more compact than normal solenoids (*3*−*7*) or different crossed-linker models (*8*−*14*) proposed for chicken erythrocyte chromatin. Here we show that a structural solution that allows the formation of compact fibers consists of the interdigitation of the successive turns of simple helices with few nucleosomes per turn.

Construction of Compact Interdigitated Helices. Three-dimensional models of chromatin fibers were constructed by using the geometric modeling system DMI (Departament de Llenguatges i Sistemes Informàtics, Universitat Politècnica de Catalunya) on a Hewlett-Packard 9000/720 workstation. All models were analyzed interactively in three dimensions in order to detect steric interferences; only structures without interferences were selected. We have used the overall dimensions of the nucleosome core (Figure 1D) obtained in X-ray crystallographic studies (*15*−*18*). Due to the wedge-shaped structure of the histone octamer (*19*−*21*), histones are almost completely hidden by DNA in the nucleosome. This shape facilitates the packaging of nucleosomes in the models proposed in this study. According to the observed helical structure and the radial bars detected in the top view of folded chromatin fragments (*1*), nucleosomes are radially distributed in all models and core particle dyad axes are orthogonal to the fiber axis.

Early work performed with space-filling models built to scale showed us that, to construct a helix of nucleosomes that (i) must be very compact (*1*) and (ii) has to be initiated and stabilized with a basic element containing about 6 nucleosomes (*2*), it is necessary to interdigitate the nucleosomes of the successive helical turns. Compact helices, with a small pitch, can be constructed using a relatively large number of nucleosomes per turn, but we have excluded this possibility because these helices require more than 6 nucleosomes to be initiated. Successive turns of a simple helix (primary helix) can interdigitate if they have a nonintegral number of nucleosomes per turn, and the diameter of the resulting structure and nucleosome tilt relative to the fiber axis give enough space for the secondary helices produced as a consequence of interdigitation. Several steps in the construction of an interdigitated helix can be seen in Figure 1 (panels A−C). This figure shows models having 2.80 (E), 3.76 (G), 4.74 (C, F), and 5.77 (H) nucleosomes per turn in the primary helix. All of these structures have secondary helices with a pitch much larger than that of the primary helices responsible for their formation. Primary and secondary helices of the models shown in Figure 1 are left-handed, but right-handed models can also be constructed (not shown). Both left- and right-handed helices have been observed in chromatin fragments studied by electron microscopy (*1*). As can be seen in panels E−H, the nucleosome tilt angle is different for each model, but in all cases the values of this angle and the other parameters of primary helices maximize the face-to-face contacts of nucleosomes in secondary helices.

Although the path of linker DNA in the folded fiber is unknown (*7*, *22*, *23*), in Figure 1A−C we have included 50 bp of linker DNA with an arbitrary conformation to show

† This work was supported in part by DGICYT Grants PB92-0602 and PB95-0611. A.B. was supported by a predoctoral fellowship from the Generalitat de Catalunya.

* Corresponding author. E-mail: jr.daban@cc.uab.es.

S0006-2960(97)03117-6 CCC: $15.00
Published on Web 03/13/1998

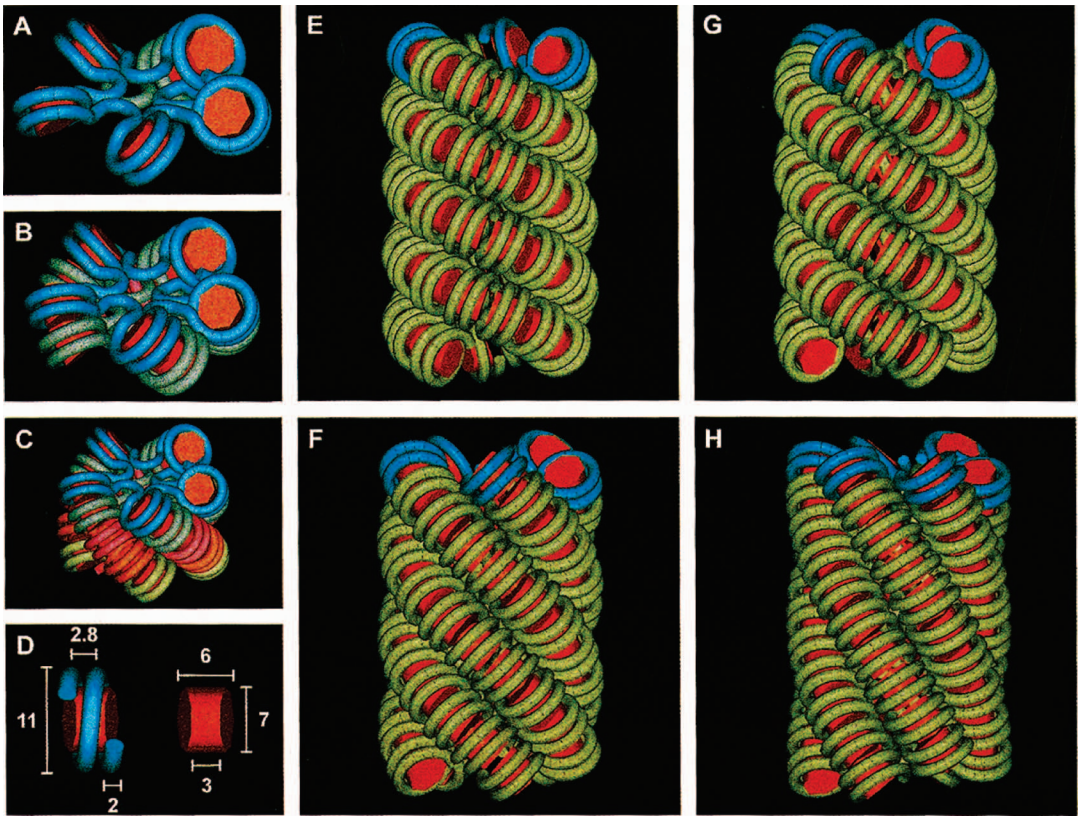

FIGURE 1: Family of interdigitated nucleosome helices. Nucleosomal DNA in the first (blue), second (gray), third (pink), fourth (orange), and fifth (green) helical turns is shown in panels A−C. These turns constitute the primary helix (4.74 nucleosomes per turn). Nucleosomes are tilted, and the successive turns of the primary helix (left-handed) are interdigitated and form five secondary helices (left-handed). Different primary helices [with 2.80 (E), 3.76 (G), 4.74 (F), and 5.77 (H) nucleosomes per turn and 2.35 (E), 3.08 (G), 3.84 (F), and 4.73 (H) nm of pitch] form interdigitated solenoids having [3 (E), 4 (G), 5 (F), and 6 (H)] secondary helices with different nucleosome tilt angles [20° (E), 29° (G), 40° (F), and 52° (H)]. In panels E−H, DNA in the first turn of the primary helices is shown in blue. The path of linker DNA is unknown and is not included in panels E−H. However, we have included linker DNA (50 bp) with an arbitrary conformation in panels A−C to facilitate the consideration of some structural aspects of the model (see text); in these panels the axis of the fiber is slightly inclined to see the linker and central hole (4 nm in diameter). All models have a diameter of 36 nm. Dimensions of the histone octamer and core particle DNA (1.8 turns of a left-handed superhelix; 146 bp; 0.34 nm/bp) are indicated (in nm) in panel D.

that this compact fiber has enough space for linker DNA. The path followed by the example of linker DNA shown in Figure 2A−C is more complex; this model contains 60 bp of linker DNA [i.e., approximately the linker length of chicken erythrocyte, 60−64 bp (*8, 14, 24*)]. Careful examination of these models in three dimensions shows that there are no steric interferences between DNA of successive helical turns. Furthermore, in agreement with our electron microscopy results showing that folded chromatin has a central hole (*1*), we have constructed our models including linker DNA with a hole in the center (Figures 1A−C and 2A,B). We have not attempted to construct structures containing two nucleosomes in the primary helix because in this case linker DNA crosses the central region and it is not possible to obtain fibers with a central hole.

The interdigitated solenoid structures presented in this study have a rise of about 0.8 nm per nucleosome. For comparative purposes, in Figure 2D,E we show a solenoid that has about the same number of nucleosomes per turn as the primary helix of the interdigitated compact structure shown in Figure 2A−C. The solenoid in Figure 2D,E has a rise per nucleosome of 2.2 nm; thus in this example the interdigitated structure is 2.7 times more tightly packaged than the corresponding solenoid without interdigitation (compare panels C and E in Figure 2).

Diameter of the Fiber Models. A limiting geometric factor for the construction of the primary helices is that their pitch has to be ≥2.0 nm to give enough space for the placement of linker DNA in the successive helical turns. This can be easily seen in the simplified linker path used in Figure 1A−C. In this case, the distance between the axes of linker DNA of first and fifth nucleosomes (Figure 1A) is 3.84 nm. In our structures, even when linker DNA has more complex conformations (as in Figure 2A), the minimum distance between the axes of linker DNA in successive turns is ≥2.0 nm. Our models do not allow the construction of helices with a pitch approaching 2.0 nm because, with such low values of pitch, the resulting secondary helices show significant steric interferences. We have avoided these interferences by increasing the helix pitch. The use of larger fiber diameters can eliminate these steric interferences without being necessary to increase the pitch. However, the experimental data available for chicken erythrocyte chromatin fibers correspond to the diameter that we have selected for the models presented in this study. Our previous electron microscopy results indicated that rotary-shadowed small chromatin fragments from chicken erythrocyte in 1.7 mM Mg^{2+} have a diameter of about 41 nm, but we estimated, after approximate correction of metal deposition, that the actual diameter is 33 nm (*1*). Since this diameter gives rise

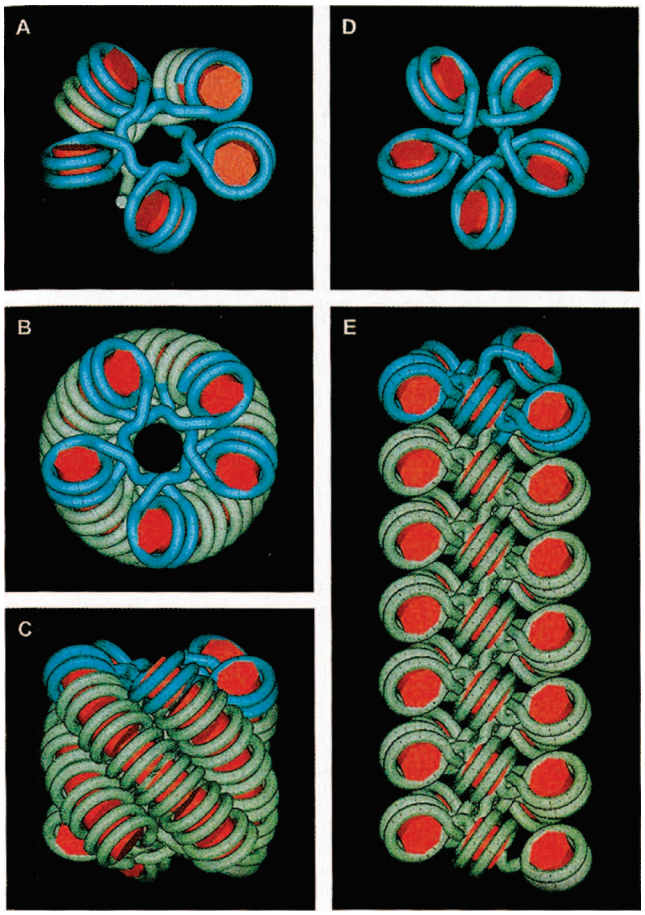

FIGURE 2: Comparison of the compactness of the interdigitated helical model (C) with a normal solenoid (E) (each structure has 35 nucleosomes drawn to the same scale). Panels B and D correspond to the top view of the structures in panels C and E, respectively. Panel A shows the complete first turn and part of the second turn of the primary helix that forms the compact fiber presented in panels B and C. The arbitrary path of the linker DNA (60 bp) used in this figure is different from that shown in Figure 1A−C, and the central hole is larger (7.3 nm in diameter). The other structural properties of the helix shown in panels A−C are equivalent to those of the model in Figure 1A−C (primary helix with 4.74 nucleosomes per turn; pitch of 3.84 nm; nucleosomes tilted 40°; and 36 nm in diameter). The solenoid shown in panel E has 5.0 nucleosomes per turn (i.e., approximately the same value as the interdigitated structure in panel C), a pitch of 11.0 nm, and nucleosomes tilted 30°; the diameters of the solenoid and central hole are 33 and 4.6 nm, respectively.

to models with a cross-sectional radius of gyration significantly lower than those found in several laboratories for folded chicken erythrocyte chromatin (see below), and since it is not possible to know exactly the thickness of the metal deposited in shadowed structures, we have used a diameter of 36 nm for the construction of all the interdigitated models presented in this work.

The cross-sectional radii of gyration, about the axis of the computer-generated models, corresponding to DNA (R_{g_D}) and core histones (R_{g_H}) were obtained directly by the program DMI. We have found 12.3 and 12.1 nm for R_{g_D} of models in Figures 1C and 2C, respectively; R_{g_H} is 12.7 nm in both models. For the solenoid in Figure 2E we have found 10.7 and 11.3 nm for R_{g_D} and R_{g_H}, respectively. To estimate the radius of gyration of models including histone H1, we have used the cross-sectional radius of gyration of histone H1 ($R_{g_{H1}}$) in chicken erythrocyte chromatin determined by Graziano et al. (*25*) by neutron scattering in 85 mM NaCl. The value of $R_{g_{H1}}$ found by these authors is 6.7−7.3 nm; we used 7.0 nm in our calculations. To calculate the radius of gyration of the whole structure (R_{g_C}), and to compare the obtained values with results found using X-ray and neutron scattering in several laboratories, it was necessary to take into account the relative contribution to the scattering of histones and DNA (*26*). Considering that histones and DNA are distributed concentrically about the axis of the solenoid, the radius of gyration of the cross section of the whole structure is

$$R^2_{g_C} = (\Delta\rho_D V_D/\sum\Delta\rho_i V_i)R^2_{g_D} + (\Delta\rho_H V_H/\sum\Delta\rho_i V_i)R^2_{g_H} + (\Delta\rho_{H1} V_{H1}/\sum\Delta\rho_i V_i)R^2_{g_{H1}}$$

where $\sum\Delta\rho_i V_i = \Delta\rho_D V_D + \Delta\rho_H V_H + \Delta\rho_{H1} V_{H1}$ and $\Delta\rho_D$, $\Delta\rho_H$, $\Delta\rho_{H1}$ and V_D, V_H, V_{H1} are contrast and volume of DNA, core histones, and histone H1, respectively. To calculate contrast corresponding to X-ray and neutron scattering, the electron densities and scattering length densities used for DNA, core histones (and H1), and water were respectively 0.51, 0.44, and 0.33 e/Å^3 (*9*) and 0.38 × 10^{11}, 0.20 × 10^{11}, and −0.06 × 10^{11} cm^{-2} (*27*). We used 139 nm^3 per core histone octamer (*19, 27, 28*) and 0.57 nm^3 per bp (*27*), respectively, to calculate V_H and V_D of the models. The value of V_{H1} (33.9 nm^3 per molecule of H1) was estimated by considering the molecular mass ratio of the histone H1 to core histone octamer (*29*).

Using the data indicated in the preceding paragraph, we have found that for each model the cross-sectional radii of gyration of the whole structure obtained using the contrast corresponding to X-rays and neutrons have the same value. The radius of gyration of folded chicken erythrocyte chromatin found by Bradbury and Baldwin (*27*), Graziano et al. (*30*), and Williams and Langmore (*24*) ranges from 12.1 to 12.5 nm. The radii of gyration found for the interdigitated compact models of Figures 1C and 2C including histone H1 are, respectively, 12.1 and 12.0 nm. Thus the diameter of 36 nm used in our models is in agreement with the experimental values found in several laboratories for chicken erythrocyte chromatin in 1.2 mM Mg^{2+} (*27*) or 75−80 mM Na^+/K^+ (*24, 30*). Normal solenoid (Figure 2E) has a calculated radius of gyration of 10.6 nm. This value is similar to that found experimentally (*27*) at lower ionic strength (40 mM NaCl). Other authors have found low values (∼10 nm) for the radius of gyration of chicken erythrocyte chromatin even in the presence of Mg^{2+} (*31*) or intermediate concentrations of NaCl (*32*). Recently, Graziano et al. (*25*) have found that the cross-sectional radius of gyration of chicken erythrocyte chromatin in 85 mM NaCl without the contribution of H1 is 12.2 nm. In keeping with this experimental value, our results show that the model including a hole of 7.3 nm in diameter and 60 bp of linker DNA (Figure 2C) has a radius of gyration calculated without H1 of 12.3 nm.

Compactness of Interdigitated Nucleosome Helices. Relationship to Other Models. In the typical solenoid model there are about 6 nucleosomes per 11 nm (*3, 6, 7*). Bradbury and Baldwin (*27*), from neutron scattering studies of chicken erythrocyte chromatin in 1.2 mM Mg^{2+}, have suggested a relatively compact solenoidal structure containing 8.8 nu-

cleosomes per 11 nm. A crossed-linker model with 6 nucleosomes per 11 nm based on X-ray scattering results obtained with chicken erythrocyte chromatin in the presence of Mg^{2+} has been proposed by Koch and co-workers (*9, 10, 31*). Makarov et al. (*33*) have proposed a triple helix model with crossed linker containing about 7 nucleosomes per 11 nm. A more compact crossed-linker model has been proposed by Williams et al. (*8*); in this model for chicken erythrocyte chromatin in 75 mM Na^+/K^+ the mass per unit length corresponds to 9.1 nucleosomes per 11 nm as determined by X-ray scattering (*24*). Finally, Woodcock et al. (*34*) using scanning transmission electron microscopy obtained a mass per unit length corresponding to 11.6 nucleosomes per 11 nm for chicken erythrocyte chromatin in 150 mM NaCl and suggested a compact zigzag ribbon model with a helical repeat of about 18 nucleosomes. Although this model is compact, it is not consistent (i) with our previous results showing that 5−7 nucleosomes are enough to form the basic structure of folded chicken erythrocyte chromatin (*1, 2*) and (ii) with results obtained in sedimentation studies indicating a marked transition when the fragments analyzed contain about 6 nucleosomes (*35*). The family of interdigitated solenoids of this work (Figure 1E−H) is formed from an initial structure containing 3−6 nucleosomes and has 13−14 nucleosomes per 11 nm.

The rise per nucleosome obtained with the interdigitated models is low (0.82 nm per nucleosome) but is significantly higher than the value found in our previous electron microscopy study [0.43 nm per nucleosome (*1*)]. Although part of the apparent compaction may be due to distortion of chromatin fragments adsorbed on the electron microscopy grids, the possibility that the interdigitated solenoids could be more compact than the models presented in this study must be considered. First, since the models have been constructed avoiding completely all kinds of steric interferences, the resulting structures do not show the maximum compactness. Second, the models have been constructed without considering that the actual shape of the histone octamer is a distorted wedge (*19*−*21*) that can facilitate a closer approach between the nucleosomes stacked in the secondary helices. Finally, DNA molecules can have an effective radius lower than 2.0 nm when they are packed in supramolecular assemblies (*36*), and this could also produce a higher degree of compaction of actual fibers.

Structural Implications of Secondary Helices. In contrast with the interdigitated model, in the normal solenoid structure (*3, 6, 7*) contacts between successive turns of the helix occur exclusively through nucleosome edges, and there is no formation of secondary helices. In some models different degrees of overlapping of nucleosomes have been described (*8*−*10, 31, 33*). The high compactness of the interdigitated model can only be obtained if the stacking of nucleosomes in the secondary helices is maximum. This is completely compatible with early results obtained in several laboratories showing that core particles have a strong tendency to interact through their faces (*37*) forming arcs and helices (*38, 39*). The bending of linker DNA observed by Yao et al. (*40*) in dinucleosomes depleted of H1 could also be caused by this interaction. Recent results of Luger et al. (*18*) showing the existence of extended histone amino-terminal tails in core particle crystals suggest that histone tails could be involved in the formation of these complexes. The stacking of nucleosome cores in secondary helices is also in agreement with cross-linking (*41*) and electron microscopy (*19, 42, 43*) results demonstrating that histone octamers can associate, forming different oligomers of higher molecular mass and aggregated helical tubes. The stabilization given by these interactions could be responsible for the folding and self-assembly of chromatin fragments containing few nucleosomes found in electrophoretic studies (*2*). In our models the first turn is sealed when the fourth (Figure 1E), fifth (Figure 1G), sixth (Figures 1A,F and 2A), or seventh (Figure 1H) nucleosome interacts with the first nucleosome.

We have observed that, for a fixed diameter, the higher the number of nucleosomes per turn of the primary helix the higher the nucleosome tilt angle necessary to form secondary helices without steric interferences (see legend of Figure 1). However, since electric (*4, 44*) and photochemical (*45*) dichroism studies have indicated tilt angles between 20° and 38°, it seems that compact chromatin containing more than 5 nucleosomes per turn of the primary helix is unlikely to exist in actual fibers. Furthermore, the meridional 11 nm diffraction found in X-ray studies of partially oriented chicken erythrocyte chromatin fibers (*6*) also suggests that nucleosome tilt angles cannot be high. Finally, the secondary helices formed in interdigitated structures could be responsible for the cross-striations seen by different authors (*3, 8, 34*) in folded chromatin fibers. Since the pitch angles of the helices suggested by these authors are relatively low, it can be considered again that the models containing more than 5 nucleosomes in the primary helix are less consistent with the experimental data.

Structural Flexibility. According to Widom (*7*), the study of the structure of completely folded chromatin has been difficult because using different techniques it has been found that chromatin structures continue to change even past the point of bulk precipitation. The compact helical structures found in our electron microscopy studies (*1*) could correspond to a final folded state of chromatin that cannot be studied using other experimental approaches due to precipitation problems. The microscopy studies of Subirana et al. (*12*), Woodcock et al. (*13*), and Leuba et al. (*14*) have indicated that extended chromatin fibers are irregular. Irregularities are particularly visible at low ionic strength (*14*), but even fibers compacted at higher ionic strength are irregular and segmented (*46*). Fiber stabilization produced by stacking of nucleosomes in secondary helices, and by contacts between nucleosome edges in successive helical turns, could favor folding of the irregular extended fibers into compact interdigitated helices. Due to technical limitations of our computer modeling system, the family of interdigitated models have been generated using regular geometric parameters and correspond to idealized structures that do not represent the intrinsic irregularities of chromatin. In keeping with a previous observation of Woodcock et al. (*34*), the differences between the number of nucleosomes per unit length found in our electron microscopy studies and in solution studies in the presence of Mg^{2+} could be due in part to the fact that in solution studies the heterogeneity and discontinuities of the fibers may reduce the apparent values of the mass per unit length of the compact regions of chromatin. Since it has been found that there is a correlation of the fiber diameter with the mass per unit length (*27, 47*),

it can be suggested that the typical solenoid is an idealized, and relatively compact, intermediate structure that can fold by interdigitation, giving rise to more compact structures with a higher diameter. The discontinuities in native folded fibers seen in the electron microscope suggest that this final folded structure can only be regularly ordered in relatively short regions.

There are several lines of evidence indicating that linker DNA is extended (*23*, *48*, *49*). The arbitrary path of linker DNA in the model in Figure 2A is bent to a certain extent. However, note that since consecutive nucleosomes in the primary helices are not in contact, an intense bending of linker DNA is not required in the interdigitated models. Idealized structures presented in this work do not include linker variability. Nevertheless, linkers shorter than the mean length can be placed in the interdigitated structures if they adopt a more extended conformation; longer linkers can also be included if they occupy part of the central hole. The model has also space for H1 molecules, which according to their binding properties (*50*−*52*) and the geometry of our model have to be radially distributed, with the globular part at a distance of 6.5 nm from the fiber axis as determined by Graziano et al. (*25*). In studies performed with chromatin from different species, it has been found that the diameter of chromatin fibers increases with DNA linker length (*8*, *24*). The increase of diameter in our models will produce fibers with a larger number of nucleosomes per unit length. This is in agreement with results indicating that the mass per unit length is dependent on linker length (*8*, *24*). These structural variations can be absorbed by the interdigitated solenoids because, presumably, according to the study of Dubochet and Noll (*39*) about the structure of helices formed by the face-to-face association of nucleosome core particles, the stacks of nucleosomes in secondary helices can adopt a wide range of shapes.

According to Kellenberger et al. (*53*) the degree of compactness of DNA in a biological structure can be described by the local concentration of DNA within the structure. The local concentration of DNA in metabolically inert structures such as phage heads (*53*, *54*) and insect sperm (*55*) is about 0.9 g/mL. The local concentration of DNA in the normal solenoid structure is significantly lower, about 0.15 g/mL. It can be speculated that this loss of efficiency in the use of space is necessary for the rapid access of the cellular machinery to the genetic information. The interdigitated helical structure described in this study has a relatively high local concentration of DNA, about 0.3 g/mL. Note, however, that DNA within this compact structure follows essentially the simple pattern of successive supercoiling of the normal solenoid and can easily unfold, giving rise to extended fibers in active chromatin.

ACKNOWLEDGMENT

We thank Iñigo Gurrea and Dr. Lluis Solano (Departament de Llenguatges i Sistemes Informàtics, UPC) for excellent technical help and advice in the use of the program DMI and Dr. S. Bartolomé (Laboratori d'Anàlisi i Fotodocumentació, UAB) for help in the preparation of the figures.

REFERENCES

1. Bartolomé, S., Bermúdez, A., and Daban, J.-R. (1994) *J. Cell Sci. 107*, 2983.
2. Bartolomé, S., Bermúdez, A., and Daban, J.-R. (1995) *J. Biol. Chem. 270*, 22514.
3. Finch, J. T., and Klug, A. (1976) *Proc. Natl. Acad. Sci. U.S.A. 73*, 1897.
4. McGhee, J. D., Nickol, J. M., Felsenfeld, G., and Rau, D. C. (1983) *Cell 33*, 831.
5. Butler, P. J. G. (1984) *EMBO J. 3*, 2599.
6. Widom, J., and Klug, A. (1985) *Cell 43*, 207.
7. Widom, J. (1989) *Annu. Rev. Biophys. Biophys. Chem. 18*, 365.
8. Williams, S. P., Athey, B. D., Muglia, L. J., Schappe, R. S., Gough, A. H., and Langmore, J. P. (1986) *Biophys. J. 49*, 233.
9. Bordas, J., Perez-Grau, L., Koch, M. H. J., Vega, M. C., and Nave, C. (1986) *Eur. Biophys. J. 13*, 175.
10. Koch, M. H. J. (1989) in *Protein*−*Nucleic Acid Interaction* (Saenger, W., and Heinemann, U., Eds.) pp 163−204, Macmillan Press, London.
11. Staynov, D. Z. (1983) *Int. J. Biol. Macromol. 5*, 3.
12. Subirana, J. A., Muñoz-Guerra, S., Aymamí, J., Radermacher, M., and Frank, J. (1985) *Chromosoma 91*, 377.
13. Woodcock, C. L., Grigoryev, S. A., Horowitz, R. A., and Whitaker, N. (1993) *Proc. Natl. Acad. Sci. U.S.A. 90*, 9021.
14. Leuba, S. H., Yang, G., Robert, C., Samori, B., van Holde, K., Zlatanova, J., and Bustamante, C. (1994) *Proc. Natl. Acad. Sci. U.S.A. 91*, 11621.
15. Richmond, T. J., Finch, J. T., Rushton, B., Rhodes, D., and Klug, A. (1984) *Nature 311*, 532.
16. Uberbacher, E. C., and Bunick, G. J. (1989) *J. Biomol. Struct. Dyn. 7*, 1.
17. Struck, M.-M., Klug, A., and Richmond, T. J. (1992) *J. Mol. Biol. 224*, 253.
18. Luger, K., Mäder, A. W., Richmond, R. K., Sargent, D. F., and Richmond, T. J. (1997) *Nature 389*, 251.
19. Klug, A., Rhodes, D., Smith, J., Finch, J. T., and Thomas, J. O. (1980) *Nature 287*, 509.
20. Arents, G., Burlingame, R. W., Wang, B.-C., Love, W. E., and Moudrianakis, E. N. (1991) *Proc. Natl. Acad. Sci. U.S.A. 88*, 10148.
21. Arents, G., and Moudrianakis, E. N. (1993) *Proc. Natl. Acad. Sci. U.S.A. 90*, 10489.
22. van Holde, K., and Zlatanova, J. (1995) *J. Biol. Chem. 270*, 8373.
23. van Holde, K., and Zlatanova, J. (1996) *Proc. Natl. Acad. Sci. U.S.A. 93*, 10548.
24. Williams, S. P., and Langmore, J. P. (1991) *Biophys. J. 59*, 606.
25. Graziano, V., Gerchman, S. E., Schneider, D. K., and Ramakrishnan, V. (1994) *Nature 368*, 351.
26. Serdyuk, I. N. (1979) *Methods Enzymol. 59*, 750.
27. Bradbury, E. M., and Baldwin, J. P. (1986) *Cell Biophys. 9*, 35.
28. Uberbacher, E. C., Harp, J. M., Wilkinson-Singley, E., and Bunick, G. J. (1986) *Science 232*, 1247.
29. von Holt, C., Brandt, W. F., Greyling, H. J., Lindsey, G. G., Retief, J. D., Rodrigues, J. de A., Schwager, S., and Sewell, B. T. (1989) *Methods Enzymol. 170*, 431.
30. Graziano, V., Gerchman, S. E., and Ramakrishnan, V. (1988) *J. Mol. Biol. 203*, 997.
31. Koch, M. H. J., Vega, M. C., Sayers, Z., and Michon, A. M. (1987) *Eur. Biophys. J. 14*, 307.
32. Greulich, K. O., Wachtel, E., Ausio, J., Seger, D., and Eisenberg, H. (1987) *J. Mol. Biol. 193*, 709.
33. Makarov, V., Dimitrov, S., Smirnov, V., and Pashev, I. (1985) *FEBS Lett. 181*, 357.
34. Woodcock, C. L. F., Frado, L.-L. Y., and Rattner, J. B. (1984) *J. Cell Biol. 99*, 42.
35. Thomas, J. O., and Butler, P. J. G. (1980) *J. Mol. Biol. 144*, 89.
36. Timsit, Y., and Moras, D. (1994) *EMBO J. 13*, 2737.
37. Tatchell, K., and van Holde, K. E. (1978) *Proc. Natl. Acad. Sci. U.S.A. 75*, 3583.
38. Finch, J. T., Lutter, L. C., Rhodes, D., Brown, R. S., Rushton, B., Levitt, M., and Klug, A. (1977) *Nature 269*, 29.
39. Dubochet, J., and Noll, M. (1978) *Science 202*, 280.

40. Yao, J., Lowary, P. T., and Widom, J. (1991) *Biochemistry 30*, 8408.
41. Thomas, J. O., and Kornberg, R. D. (1975) *Proc. Natl. Acad. Sci. U.S.A. 72*, 2626.
42. Sperling, R., and Wachtel, E. J. (1981) *Adv. Protein Chem. 34*, 1.
43. Greyling, H. J., Schwager, S., Sewell, T., and von Holt, C. (1983) *Eur. J. Biochem. 137*, 221.
44. Yabuki, H., Dattagupta, N., and Crothers, D. M. (1982) *Biochemistry 21*, 5015.
45. Mitra, S., Sen, D., and Crothers, D. M. (1984) *Nature 308*, 247.
46. Zlatanova, J., Leuba, S. H., Yang, G., Bustamante, C., and van Holde, K. (1994) *Proc. Natl. Acad. Sci. U.S.A. 91*, 5277.
47. Gerchman, S. E., and Ramakrishnan, V. (1987) *Proc. Natl. Acad. Sci. U.S.A. 84*, 7802.
48. Bednar, J., Horowitz, R. A., Dubochet, J., and Woodcock, C. L. (1995) *J. Cell Biol. 131*, 1365.
49. Pehrson, J. R. (1995) *J. Biol. Chem. 270*, 22440.
50. Goytisolo, F. A., Gerchman, S. E., Yu, X., Rees, C., Graziano, V., Ramakrishnan, V., and Thomas, J. O. (1996) *EMBO J. 15*, 3421.
51. Pruss, D., Bartholomew, B., Persinger, J., Hayes, J., Arents, G., Moudrianakis, E. N., and Wolffe, A. P. (1996) *Science 274*, 614.
52. Crane-Robinson, C. (1997) *Trends Biochem. Sci. 22*, 75.
53. Kellenberger, E., Carlemalm, E., Sechaud, J., Ryter, A., and de Haller, G. (1986) in *Bacterial Chromatin* (Gualerzi, C. O., and Pon, C. L., Eds.) pp 11−25, Springer-Verlag, Berlin.
54. Kellenberger, E. (1987) *Trends Biochem. Sci. 12*, 105.
55. Suzuki, M., and Wakabayashi, T. (1988) *J. Mol. Biol. 204*, 653.

BI973117H